An Efficient Microwave-Assisted Synthesis Method of Novel Bi_2O_3 Nanostructure and Its Application As a High-Performance Nanocatalyst in Preparing Benzylidene Barbituric Acid Derivatives

Mahdieh Yahyazadehfar
Islamic Azad University Kerman Branch
Enayatollah Sheikhhosseini (sheikhhosseiny@gmail.com)
Islamic Azad University Kerman Branch https://orcid.org/0000-0003-2973-9768
Sayed Ali Ahmadi
Islamic Azad University Kerman Branch
Dadkhoda Ghazanfari
Islamic Azad University Kerman Branch

Nano Express

Keywords: Bi2O3 nanostructure, Efficient synthesis route, Novel catalyst, Benzylidene barbituric acid

Posted Date: October 18th, 2021

DOI: https://doi.org/10.21203/rs.3.rs-966810/v1

Abstract

In this study, controllable and optimal microwave irradiation has been used to synthesize the novel nanostructures of Bi_2O_3 under environmental conditions. The final products had a thermal stability of 210 °C, an average particle size distribution of 85 nm, and surface area of 783 m^2/g. The high thermodynamic stability of Bi_2O_3 nanostructures were confirmed by TG and DSC analyses. The nanostructure nature of compounds, most importantly, the use of effective, cost effective and rapid synthesis route of microwave have created significant physiochemical properties in the Bi_2O_3 products. These unexpected properties have made the possibility of potentials application of these products in various fields, especially in nanocatalyst applications. It is well-documented that, as Lewis acid, bismuth nanocatalyst exhibits a great catalytic activity for the green synthesis of some bio-active barbituric acid derivatives using precursors with electron-donating or –withdrawing nature in high yields (80-98%). After incorporating this catalyst into the aqueous media, all the reactions were completed within 2-3 min at room temperature. The main advantages of this method are practical facility, the availability of starting materials, and low costs besides the catalyst reusability. Additionally, the catalyst synthesis process may be carried in the aqueous media during a short period with medium to high yields. The obtained results have opened a new window for development of a novel nanocatalyst with practical application.

Introduction

Bi_2O_3 nanostructures are one of the most important products from transition metal oxides [1]. These structures, because of having special properties, attracted particular attention to themselves in recent decade [2]. Among their extraordinary properties, the dielectric, piezoelectric, corrosion resistance, environmental compatibility and low-cost properties can be mentioned [3–5]. The surface and physic-chemical natures of Bi_2O_3 is such that electron transfers are easily exchanged between photo-generated and electron-hole pairs and as a result, these compounds can be used as a critical nanostructure in various fields [6, 7].

Metal oxide nanostructures are produced by various methods, among which hydrothermal [8], ultrasonic [9], sol-gel and other conventional methods [10] can be mentioned. Many of these methods require specific conditions that not only cause the reactions under controlled conditions, but also leave many environmental impacts.

In order to overcome these problems, the microwave route has been proposed as an effective method to prepare of various structures. Among the advantages of this method, it can be mentioned that the time duration of the synthesis process is reduced. The reactions are also carried out under low temperature, and carbon dioxide emission is reduced compared to other methods. In addition, the major difference in using microwave irradiation compared to other conventional methods is that in the usual methods, at first, heat is irradiated to the surface of the material and then it is transmitted to the inside of the bulk. But in microwave methods, electromagnetic energy directly enters the structure of material. As a result of homogeneous irradiation of heat, the optimum use of energy is made, which creates desirable physiochemical properties in the structure.

As a cyclic-amide, barbituric acid is the raw material in the synthesis of barbiturates. The mixtures of the derivatives of this material with alkyls and aryls exhibits hypnotic and seductive effects [11] Several derivatives of 5-arylidene barbituric acid have been more concerned as the raw material, which encompass the intermediate in the synthesis of benzyl barbituric derivatives [12] as well as heterocyclic compounds [13] asymmetrical disulphides [11] oxadiazaflavines [14]. Moreover, these derivatives have been extensively exploited in the pharmaceutical industry as anesthetics and central nervous system depressants [15, 16], local anaesthetic ,antispasmodic, sedative, hypnotic [17], antimicrobial, antifungal, antitumor [18], anticonvulsant [19] and anticancer [20], as well as complex and salt formation reagent [21–25], analgesic, bronchodilator, vasodilator, anti-parkinsonian, antimalarial and anti-allergic agents [26–30].

Various synthetic methods have been introduced for the preparation of 5-arylidene barbituric acid derivatives, in which different catalysts, including solvent free grinding using NH_2SO_3H [31] microwave irradiation [32] an infra-red promoted route [33] and condensation using ionic liquid media [34] are employed.

Although some researchers have reported this reaction with the use of no catalyst [35, 36], the following catalysts are used and introduced in this regard: [DABCO]$(SO_3H)_2Cl_2$ [37], [DABCO] $(SO_3H)_2(HSO_4)_2$ [38], *p*- nanoporous MMT-$HClO_4$ [39], dodecylbenzenesulfonic acid (DBSA) [40], $FeCl_3.6H_2O$ [41] ethylammonium nitrate [42], silico-tungstic acid [43], amino-sulfonic acid [31], NaOH/fly ash [44], sodium *p*-toluene sulfonate (NaPTSA) [45], $CoFe_2O_4$-NPs [46], non-catalyst/infrared irradiation [33], BF_3/nano γ-Al_2O_3 [47] succinimidinium N-sulfonic acid hydrogen sulfate ([SuSA-H]HSO_4) [48], basic alumina [49], Verjuice [50], sulfonic acid functionalized nanoporous silica (SBA-Pr-SO_3H) [37], copper oxide nanoparticles (CuO-NPs) [51], aminosulfonic acid (NH_2SO_3H) [31], 2-amino-3-(4-hydroxyphenyl) propanoic acid (*L*-tyrosine) [52], $CoFe_2O_4$ nanoparticles [46], sodium acetate (CH_3COONa) [53], 1-n-butyl-3-methylimmidazolium tetrafluoroborate ([bmim]BF_4) [34], polyvinyl pyrrolidone stabilized nickel nanoparticles (PVP-Ni-NPs) [54], cetyltrimethyl ammonium bromide (CTMAB) [55], ethyl ammonium nitrate (EAN) [42], ZrO_2/SO_4^{-2} [56], sodium *p*-toluene sulfonate (NaPTSA) [45], $Ce_1MgxZr_{1-x}O_2$ (CMZO) [57], taurine [58]. The methods adopted to produce these heterocyclic compounds have been useful and effective; however, the methods also have their own disadvantages and drawbacks, including expensive catalysts and reagents, harsh conditions for the catalyst synthesis, the use of contaminated organic solvents and/or corrosive inorganic acids, tedious laboring, non-reusability of the catalyst, and the need for extra amounts of this reagent or the others as well as the incorporation of self-condensation and bis-addition.

Using water as the reaction medium, in addition to providing the advantage of organic synthesis in an aqueous medium, directs the procedure toward a more environmentally-benign path. Moreover, in situ reductant generation decreases the purification steps and the waste generation, which facilitates the procedure and makes it more practical.

Cobalt nanocatalyst has been utilized successfully so that it leads to the desirable results in the synthesis of arylidene barbituric acid derivatives.

In this work, novel nanostructures of Bi_2O_3 products are prepared under microwave irradiations with ideal physiochemical properties. For this purpose, final nanostructures were characterized by relevant analyses, and the microwave process was optimized to select the desired products. Finally, the practical

application of these nanostructures was investigated in the nanocatalyst reaction of preparation benzylidene barbituric acid derivatives.

Experimental

Chemicals and reagent

$Al_2O_3.4SiO.H_2O$ (MW: 224.145 g/mol, 99.99%), Bi $(NO_3)_3.5H_2O$ (MW: 485.0715 g/mol, 99.98%) as well as barbituric acid and aromatic aldehyde derivatives were supplied from Merck Chemical Company. The as-received materials were used with no purification.

Material characterization

The thermodynamic behavior of the Bi_2O_3 nanostructures were analyzed with 5 K/min using Thermo-gravimetric analysis (TGA), differential scanning calorimetry (DSC) system (Netzsch QMS403C). The X-ray diffraction (XRD) patterns of the samples were analyzed on XPert PRO PANalytical diffractometer using CuKa radiations. XRD was performed at 2theta range of 10–90. The surface morphology of Bi_2O_3 nanocatalyst was evidenced from the scanning electron microscopy (SEM, Hitachi, S-4800, 25 15 kV). The Brunauer-Emmett-Teller (BET) and Barrett-Joyner-Halenda (BJH) measurements were applied using Micrometrics ASAP2010analyzer to calculate the surface area and pore-size distributions of crystals scratched from the Bi_2O_3 nanostructures. The magnetic hysteresis loops were recorded using vibrating sample magnetometer (Changchun Yingpu, VSM-300). FT-IR spectroscopy were performed by a Perkin-Elmer FT-IR 240-C spectrophotometer (KBr). ^{13}C NMR and ^{1}H NMR (400 MHz) spectra were obtained by a Bruker Av-400 spectrometer in DMSO-d_6 using tetramethylsilane (TMS) as the internal standard. Melting points were measured using Electrotermal 9100 apparatus and were then corrected. The progress of reactions was assessed using thin layer chromatography (TLC), and the products were identified based on their melting points and IR spectra, in comparison to the authentic samples and those reported in the literature. The reaction yields were estimated with regard to the isolated products.

Catalyst preparation

In order to synthesize of Bi_2O_3 nanostructures, the solutions including 2 mmol Bi $(NO_3)_3.5H_2O$ in 10 mL ethylene glycol (Sol. a), and 2 mmol $Al_2O_3.4SiO.H_2O$ in 10 mL ethylene glycol (Sol. *b*) were separately prepared under environmental conditions. The obtained solution (Sol. a and Sol. **b**) was stirred at temperature of 60°C for a period of 20 min. The obtained mixture has been entered into a microwave reactor and has been placed under the optimal conditions of 120 W for time duration of 15 min at microwave temperature of 26°C. Calcinations` procedure were then performed on the sample so that a pure Bi_2O_3 nanostructure was created. At the end, the products were washed three times with distilled water to eliminate impurities existing in the structure. Also, in order to dry the products, they have been placed in the oven up to 80° C. After 2 h, the primary nuclei related to the formation of Bi_2O_3 nanocrystals were formed.

General procedure for the preparation of benzylidene barbituric acid derivatives: A mixture of barbituric acid (1 mmol), aldehyde (1 mmol) and 20 W% (0.029 g) Bi_2O_3 nanocatalyst in water (10 mL) was stirred at room temperature. The completion of the reaction was monitored by TLC [ethyl acetate: n-hexane (4:6)]. To gain pure benzylidene barbituric acid derivatives, when the reaction was completed, the mixture was filtered, and the solid retentate was washed three times with 10 mL water.

Results And Discussion

Charactrization of Bi_2O_3 nonocatalyst

Thermodynamic and nanocrystalline behaviors

Figure 1a. shows the thermodynamic behaviour of Bi_2O_3 samples from environment temperature up to 700°C. Based on TG analysis, four observable peaks have been presented. The peak at temperature of 60°C was related to evaporation of surface water. In the second stage (91°C), the impurities and solvents trapped in the network were vanished. In order to create a pure Bi_2O_3 sample, it was better to heated up the samples to this temperature range. A considerable weight reduction occurred within the temperature of 214°C, which can be attributed to the destruction of the B_2O_3 sample. The remaining sample components also collapsed at 368°C.

Based on DSC curve, the presence of endothermic peaks showed the energies required for weight reduction of the Bi_2O_3 sample components in each one of the mentioned stages. Since each one of the DSC peaks was in accordance with the TG data, therefore, the product had not undergone phase change in the above temperature range [59]. These results were consistent with the XRD data that confirmed the presence of pure single phase in the Bi_2O_3 sample.

The XRD patterns of the nanostructures have been presented in Figure 1b. The diffracted peaks indicated that the sample has been indexed in the BCC system with the Bi_2O_3 crystalline phase (JCPDS No. 34-0097) [60].

Based on the results, no peaks related to the presence of impurity or the formation of multiple phases has been observed, which confirmed the successful synthesis of the pure structure of Bi_2O_3 samples. The presence of some sharp peaks indicated that the samples had a high crystalline structure [61]. As a result, the effective microwave route affected the formation of Bi_2O_3 nanocatalyst with high purity and significant crystalline percentages (Fig. 1).

Morphology And Size Distribution

The morphology and particle size distribution of Bi_2O_3 sample with various magnifications have been shown in Figure 2a and b. According to these images, the SEM micrographs confirmed the formation of Bi_2O_3 crystals with tiny sizes. The size of crystals was in the nanometric range, which was in accordance

with the XRD results. Also, SEM results showed that the surface morphology of both samples was plate-like nanostructures and particles have been distributed uniformly without any evidence of agglomeration. In addition, the Bi_2O_3 samples showed a dense surface with good connections between the crystals (Fig. 2).

Textural and magnetic properties

The N_2 adsorption/desorption isotherm and the porosity of Bi_2O_3 nanocatalyst synthesized under optimal conditions of microwave irradiation has been exhibited in Figure 3a and b, respectively. According to classical isotherms [62], Bi_2O_3 sample had the adsorption/ desorption behavior similar to the type IV isotherms, which indicated the mesoporous size distribution for them [63]. Based on the BJH method, the Bi_2O_3 samples also had an average pore size distribution of 4 nm, which was in accordance with the type IV isotherms. According to the results obtained from BET technique, the sample had a surface area of about 783 m^2/g [64], which was considerable compared to the previous samples. The increase of surface area and porosity of the products can be attributed to the desirable conditions of nucleation, growth of crystals, as well as the effective impact of microwave synthesis parameters (Fig. 3) [65].

Figure 4 exhibits the magnetic hysteresis of the Bi_2O_3 nanostructures prepared by microwave route under optimal condition. The saturation magnetization of this novel nanocatalyst is about 65/4 emu/g. Also, it displays a small coercivity along with narrow hysteresis that confirmed the soft magnetic properties for this samples. This can be related to the results of small crystalline size of Bi_2O_3 nanostructure that approved the inversely relation between coercivity and size distribution by D6 [66].

Synthesis of benzylidene barbituric acid using Bi_2O_3 nanoparticles

This project mainly aimed to synthesize recyclable bismuth oxide nanoparticles using a facile, high-performance and pro-environmental method. The nanoparticles were used as the catalyst in the production process of the arylidene barbituric acid derivatives (Scheme 1).

The performance of Bi_2O_3 nanocatalyst was investigated using barbituric acid (2) and 4-chlorobenzaldehyde (1j), as the model substrate. In order to optimize the reaction conditions, various weight percentage of catalyst and diverse solvents were exploited.

Firstly, the model reaction was performed solvent-free with no catalyst. As expected, the reaction did not happen noticeably. In addition, in another test, no reaction happened in the absence of the solvent and the presence of the catalyst (Table 1, Entry 1, 2). Afterwards, with the use of the catalyst (20 Wt%) and several solvents, which were different in terms of polarity and protic nature, such as methanol, ethanol, C_2H_5OH/H_2O, chloroform, toluene, dichloromethane, and acetonitrile, the reaction was re-assessed. Monitoring the reaction revealed that the polar solvents such as methanol, ethanol, and acetonitrile were much effective than the non-polar ones. This might be attributed to the much better dispersion of the catalyst as well as much better solubility of the reagents in the polar solvents. In the next experiment, water as a green solvent was used and the reaction progress was assessed. It was found out that the synthesis of arylidene barbituric acid catalyzed by Bi_2O_3 nanostructure was progressed with higher yields (Table 1).

Table 1
Synthesis of **3j** in the presence of different solvents and amounts of catalyst

Entry	Catalyst (W%)	Solvent	Time (h/min)	Temp.	Yield (%)
1	—	—	N.R	r.t.	—
2	Bi_2O_3 20%	—	N.R	r.t.	—
3	—	H_2O	24 h	r.t.	33
4	Bi_2O_3 20%	H_2O	2 min	r.t.	91
5	Bi_2O_3 20%	EtOH	3 min	r.t.	40
6	Bi_2O_3 20%	EtOH/H_2O (1:1)	3 min	r.t.	36
7	Bi_2O_3 20%	CH_3OH	3 min	r.t.	35
8	Bi_2O_3 20%	CH_3CN	3 min	r.t.	32
9	Bi_2O_3 20%	$CHCl_3$	3 min	r.t.	24
10	Bi_2O_3 20%	CH_2Cl_2	3 min	r.t.	23
11	Bi_2O_3 20%	C_7H_8	3 min	r.t.	18
12	Bi_2O_3 5%	H_2O	2 min	r.t.	73
13	Bi_2O_3 10%	H_2O	2 min	r.t.	87
14	Bi_2O_3 15%	H_2O	2 min	r.t.	89
15	Bi_2O_3 25%	H_2O	2 min	r.t.	58
16	Bi_2O_3 30%	H_2O	2 min	r.t.	52
17	Bi_2O_3 35%	H_2O	2 min	r.t.	46

Optimizing the consumption of Bi_2O_3 nanocatalyst showed that its concentration plays a decisive role in the reaction efficiency as such increasing the catalyst concentration from 5 to 20 W% raised the product yield. On the other hand, the catalyst concentrations above 20 W% reduced the yield. Consequently, the optimum level of the catalyst was set as 20 W% for the reaction at room temperature (Table 1).

After optimizing the catalyst, the reactions of different aldehydes with both electron-donating and withdrawing substitutions were studied. It was noticed that the nanocatalyst can catalyze their conversion to the corresponding products in high yields during short reaction time. In fact, electron-donating and withdrawing functional groups on the aromatic ring of aldehydes have no considerable effect on their reaction's yields (Table 2).

Table 2
benzylidene barbituric acid derivatives obtained via the Knoevenagel condensation of benzaldehyde derivatives and barbituric acid usir

Entry	Ar	X	Product	Time (min)	Yield (%)[a]	\varvecm.\varvecp.(?) \varvecO\varvecb\varvecs\varvece\varvecr\varvecv\varvece\varvecd\varvecR\varvece\varvecp\var
1	$2\text{-}OHC_6H_4$-	O	3a	3	93	248-250 249-250
2	$4\text{-}MeOC_6H_4$-	O	3b	3	97	295-297 294-297
3	$2\text{-}MeOC_6H_4$-	O	3c	3	90	267-269 268-269
4	*P*-$(Me)_2NC_6H_4$-	O	3d	3	97	277-279 278-279
5	$C_6H_5CH{=}CH$-	O	3e	3	95	267-268 268
6	$4\text{-}OHC_6H_4$-	O	3f	3	98	>300 >300
7	$2\text{-}NO_2C_6H_4$-	O	3g	3	97	271-274 271-273
8	$4\text{-}NO_2C_6H_4$-	O	3h	3	76	269-271 268-270
9	$2\text{-}ClC_6H_4$-	O	3i	3	96	250-252 249-251
10	$4\text{-}ClC_6H_4$-	O	3j	3	94	298-300 298-300
11	$3\text{-}NO_2C_6H_4$-	O	3k	3	94	227-229 226-228
12	C_6H_5-	O	3l	3	96	250-252 249-252
13	3,4,5-$(OCH_3)_3C_6H_2$-	O	3m	3	98	249-250 238-250
14		O	3n	3	95	268-270 265-270
15	$2,4\text{-}Cl_2C_6H_3$-	O	3o	3	97	292-293 293-294
	4-OH-3-$OCH_3C_6H_3$-					

[a] Isolated yield.

Compared to our previous reports on the production of benzylidene barbituric acid in the presence of Co_3O_4 nanocatalyst at 90°C, the results of this experiment are quite remarkable and promising in terms of the reaction conditions (i.e., aqueous medium, room temperature and short periods of time). In most cases, the magnet was stopped as soon as the catalyst was introduced into the reaction medium, and in most cases the reaction was completed in less than 3 minutes.

All the products were identified by infrared (IR) spectroscopy, and their melting points were compared with the reference data. For more certainty, the structure of the product “3m, 3n and 3o” was verified using ^{1}H NMR spectroscopy as well.

For compound 3m, the main absorption peaks in FT-IR spectrum were appeared at the wavenumbers of 1654, 1733, 1751, 3240 and 3629 cm^{-1}, which are attributed to C=C bond, two groups of C=O stretching vibration, sp^2 C-H stretching and the secondary N-H stretching, respectively. In ^{1}H NMR spectral analyses of this compound it was observed that two characteristic singlets in δ 11.37 and 11.24 ppm for the NH groups of pyrimidine ring and other singlets at δ 8.27 and 7.84 ppm due to aromatic protons and CH=C olefin proton and aromatic protons respectively. Also, two signals for the methoxy groups appeared in δ 3.79 and 3.82 ppm. It indicated that barbituric acid was added successfully to 3,4,5-trimethoxy benzaldehyde and the compound “3m” was prepared.

5-(3,4,5-trimethoxybenzylidene)pyrimidine-2,4,6(1H,3H,5H)-trione (3m): Yield 98%. MP = 249-250 °C. IR (KBr, cm^{-1}): 3629, 3240, 1751, 1733, 1654. ^{1}H NMR (400 MHz, $CDCl_3$) δ: 3.79 (s, OCH_3), 3.82 (s, 2 OCH_3), 7.84 (s, H-Ar), 8.27 (s, 1H, CH=C), 11.24 (s, NH), 11.37 (s, NH).

5-(4-hydroxy-3-methoxybenzylidene)pyrimidine-2,4,6(1H,3H,5H)-trione (3o): Yield 97%, MP = 293-294. IR (KBr, cm^{-1}): 3277, 1748, 1696, 1664. ^{1}H NMR (400 MHz, $CDCl_3$) δ: 3.83 (s, CH_3O), 6.90 (d, J = 8.4 Hz, ArH), 7.81 (dd, *J* = 8 Hz, 1.8 Hz, H-Ar), 8.47 (d, *J* = 2 Hz, H-Ar), 8.22 (s, H-Ar), 10.56 (s, OH), 11.14 (s, NH), 11.26 (s, NH).

5-(2,4-dichlorobenzylidene)pyrimidine-2,4,6(1H,3H,5H)-trione (3n): Yield 95%. MP = 268-270 °C. IR (KBr, cm^{-1}): 3218, 1741, 1675. ^{1}H NMR (400 MHz, $CDCl_3$) δ: 7.48 (dd, *J* = 8.4, 2 Hz, H-Ar), 7.53 (dd, *J* = 8.4, 2 Hz, H-Ar), 7.81 (d, *J* = 2 Hz, H-Ar), 8.21 (s, 1H, CH=C), 11.29 (s, NH), 11.49 (s, NH).

To investigate the potential of this catalytic procedure and to fulfill the requirements of green chemistry, the catalyst reusability was evaluated with regard to the model reaction. The product of each step was dissolved in warm ethyl acetate, and the catalyst was subsequently recovered by centrifuging. In order to remove tars more efficiently from the catalyst surface, it was rinsed with H_2O twice and then used with no further purification in the next run. On the other hand, the solvent was removed by evaporation, and the product residue was gathered. The yields of four successive cycles from the first to fourth runs at

room temperature were 98%, 95%, 93%, and 90%, respectively (Table 3). The results show no significant decrease in the performance of the recovered catalyst compared to the fresh state; hence, the catalyst could be reused several times successively.

Table 3
Reusability of the catalyst in the preparation of 5-benzylidene barbituric acid derivative of 4-chlorobenzaldehyde

Run	Yield of 3n (%)
First of renewed catalyst	98
Second of renewed catalyst	95
Third of renewed catalyst	93
Fourth of renewed catalyst	90

The possible mechanism of barbituric acid and aryl aldehyde reaction, known as “Knoevenagel condensation”, is illustrated in scheme 2. The barbituric acid structure first converts to the enol form (keto-enol tautomerism in the first step) and it then attacks to the aldehyde (second step) activated by Bi_2O_3 nanocatalyst as a Lewis acid. Finally, the dehydration process leads to the final product (last step).

Comparison of the catalytic ability

With the aim of demonstrating the potential and the performance of the proposed method in preparing this type of compound, the method was compared with some other previously reported methods. Table 4 summarizes the results of the comparison. It can be noticed that this novel method is superior to many others, especially in terms of reaction time, catalyst reusability, and bio-environmental considerations.

Table 4
Comparison of various methods for the synthesis of (thio)barbituric acid

Entry	Catalyst	Amount of catalyst	Conditions	Time (min)	Yield (%)	Ref
1	BF_3/nano-γ-Al_2O_3	60 mg	Ethanol/r.t.	30	84	[48]
3	PVP-Ni Nps	100 mg	Ethylene glycole, 50°C	10-15	93	[55]
4	[bmim]BF_4	0.2 mL	Grinding-laying	120	78	[35]
5	EAN	2 mL	r.t.	180	83	[43]
7	CH_3COONa	100 mol%	Grinding	10	91	[54]
8	CMZO	200 mg	EtOH, 60-70°C	60	85	[58]
9	*P*-Dodecylbenzene sulfonic acid (DBSA)	30 mol%	H_2O, reflux	67	62	[41]
10	$[H_2\text{-pip}][H_2PO_4]_2$	5 mol%	H_2O/EtOH (1:1) 80°C	20	96	[68]
11	Taurine	20 mol%	H_2O, 90°C	9	96	[59]
12	$FeCl_3.6H_2O$	15 mol%	H_2O, reflux	35	80	[42]
13	NPs MMT-$HClO_4$	10 mg	H_2O, 70°C	4	94	[40]
14	NaPTSA/r.t.	50 mol%	r.t.	4	92	[46]
15	Verjuice	10 mL	60°C	7	96	[51]
16	$CoFe_2O_4$ NPs	1 mol%	H_2O, EtOH/r.t.	2-6	94-80	[47]
17	[SuSA-H]HSO_4	5 mol%	H_2O/ r.t.	2-12	80-98	[49]
18	Co_3O_4 nanocatalyst	20 W%	H_2O/ r.t.	3-25	98	[69]
19	Bentonite ($Al_2O_3.4SiO.H_2$)	25 mol%	90°C/H_2O	5-25	90-98	[70]
20	Bi_2O_3 nanocatalyst	20 W%	H_2O/r.t.	3	98	This work

Conclusion

In this work, an effective strategy of the microwave route has been proposed to synthesize Bi_2O_3 nanostructures with single phase over a short period of time and with optimal energy. This cost effective, efficient, and environment friendly route has created controlled properties of products that affected their catalytic

applications. The results of the related analyses indicated that the Bi_2O_3 samples had, high thermal stability, narrow particle size distribution, and a desirable surface area. These properties differentiated the Bi_2O_3 nanocatalysts developed in this study from the previous samples. The results showed that the application of optimal conditions of the microwave irradiation also affected the catalytic efficiency of the Bi_2O_3 products.

So, the prepared Bi_2O_3 nanocatalyst is introduced as an efficient nanocatalyst to catalyze the synthesis of benzylidene barbituric acid derivatives. Short reaction time, facile work-up process, recyclability of the catalyst, economical advantage and aquatic medium make this method promising. This method is attractive due to its safe and environment-friendly process.

Declarations

Acknowledgements

The author express appreciation to the Islamic Azad University (Kerman Branch), for supporting this investigation.

Authors' contributions

E.Sh. proposed the ideas, analyzed the result data and reviewed and edited the manuscript, M.Y. completed the experiment, analyzed the result data and wrote the manuscript, S.A and D.Gh played the role of consultant in the research stages. This article has been read by all authors and agreed to be published.

Funding

The authors received no specific funding for this work.

Conflict of interest

The authors declare that they have no conflict of interest.

Availability of Data and Supporting Materials

A The datasets supporting the conclusions of this article are included within the article and All data are fully available without restriction.

Competing interests

The authors declare that they have no competing interests.

Author details

Department of Chemistry, Kerman Branch, Islamic Azad University, Kerman, Iran.

References

1. Azizian-Kalandaragh Y, Sedaghatdoust-Bodagh F, Habibi-Yangjeh A (2015) Ultrasound-assisted preparation and characterization of β-Bi_2O_3 nanostructures: exploring the photocatalytic activity against rhodamine B. Superlattices Microstruct 81:151–160
2. Wang X, Feng X, Lu C, Yi G, Jia J, Li H (2018) Mechanical and tribological properties of plasma sprayed NiAl composite coatings with addition of nanostructured TiO_2/Bi_2O_3. Surf Coat Tech 349:157–165
3. Hashemi E, Poursalehi R, Delavari H (2019) Formation mechanisms, structural and optical properties of Bi/Bi_2O_3 One dimensional nanostructures prepared via oriented aggregation of bismuth based nanoparticles synthesized by DC arc discharge in water. Mat Sci Semicon Proc 89:51–58
4. Salim ET, Al-Douri Y, Al Wazny MS, Fakhri M (2014) Optical properties of Cauliflower-like Bi_2O_3 nanostructures by reactive pulsed laser deposition (PLD) technique. Sol Energy 107:523–529
5. Kumari L, Lin JH, Ma YR (2007) One-dimensional Bi2O3 nanohooks: synthesis, characterization and optical properties. J Phys Condens Matter 19:406204
6. Kim H, Jin C, Park S, Lee WI, Chin IJ, Lee C (2013) Structure and optical properties of Bi_2S_3 and Bi_2O_3 nanostructures synthesized via thermal evaporation and thermal oxidation routes. Chem Eng J 215:151–156
7. Ling B, Sun XW, Zhao JL, Shen YQ, Dong ZL, Sun LD, Li SF, Zhang S (2010) One-dimensional single-crystalline bismuth oxide micro/nanoribbons: morphology-controlled synthesis and luminescent properties. J Nanosci Nanotechnol 10:8322–8327
8. Hwang H, Shin JH, Lee KY, Choi W (2018) Facile one-pot transformation using structure-guided combustion waves of micro-nanostructured β-Bi_2O_3 to α-Bi_2O_3@ C and analysis of electrochemical capacitance. Appl Surf Sci 428:422–431
9. Zhang L, Wang W, Yang J, Chen Z, Zhang W, Zhou L, Liu S (2006) Sonochemical synthesis of nanocrystallite Bi_2O_3 as a visible-light-driven photocatalyst. Appl Catal A-Gen 308:105–110
10. Armelao L, Colombo P, Fabrizio M (1998) Synthesis of Bi_2O_3 and Bi_4 $(SiO_4)_3$ thin films by the sol-gel method. J Sol-Gel Sci Technol 13:213–217
11. Tanaka K, Chen X, Yoneda F (1988) Oxidation of thiol with 5-arylidene-1,3-dimethylbarbituric acid: application to synthesis of unsymmetrical disulfide1. Tetrahedron 44:3241-3249 (b) Sokmen BB, Ugras S, Sarikaya HY, Ugras HI, Yanardag R (2013) Antibacterial, antiurease, and antioxidant activities of some arylidene barbiturates. Biotechnol Appl Biochem 171:2030-2039

12. Frangin Y, Guimbal C, Wissocq F, Zamarlik H (1986) Synthesis of substituted barbituric acids via organozinc reagents. Synthesis 1986:1046-1050
13. Bojarski JT, Mokrosz JL, Bartoń HJ, Paluchowska MH (1985) Recent progress in barbituric acid chemistry. In Advances in heterocyclic chemistry. Academic Press 38:229–297
14. Figueroa-Villar JD, Cruz ER, Lucia dos Santos N (1992) Synthesis of oxadeazaflavines from barbituric acid and aromatic aldehydes. Synth Commun 22:1159–1164
15. Vieira AA, Gomes NM, Matheus ME, Fernandes PD, Figueroa-Villar JD (2011) Synthesis and in vivo evaluation of 5-chloro-5-benzobarbiturates as new central nervous system depressants. J Brazil Chem Soc 22:364–371
16. Balas VI, Verginadis II, Geromichalos GD, Kourkoumelis N, Male L, Hursthouse MB, Repana KH, Yiannaki E, Charalabopoulos K, Bakas T, Hadjikakou SK (2011) Synthesis, structural characterization and biological studies of the triphenyltin (IV) complex with 2-thiobarbituric acid. Eur J Med Chem 46:2835–2844
17. Jursic BS (2001) A simple method for Knoevenagel condensation of α, β-conjugated and aromatic aldehydes with barbituric acid. J Heterocycl Chem 38:655–657
18. (a) Ma L, Li S, Zheng H, Chen J, Lin L, Ye X, Qiu N (2011) Synthesis and biological activity of novel barbituric and thiobarbituric acid derivatives against non-alcoholic fatty liver disease. Eur J Med Chem 46:2003-2010 (b) Ikotun AA, Ojo Y, Obafemi CA, Egharevba GO (2011) Synthesis and antibacterial activity of metal complexes of barbituric acid. Afr J Pure Appl Chem 5:97-103 (c) Beres JA, Coons TL, Kaelin MJ (1974) Synthesis and antibacterial properties of substituted decylbarbituric acids. J Pharm Sci 63:469-471 (d) Kidwai M, Thakur R, Mohan R (2005) Ecofriendly synthesis of novel antifungal (thio) barbituric acid derivatives. Acta Chim. Slov 52:88-92 (e) Gulliya KS (1999) Uses for barbituric acid analogs. US Pat 5:869,494
19. Goodman LS, Gilman A (1991) The Pharmacological Basis of Therapeutics; Mc Graw-Hill: New Delhi, India, 1991: 358–360
20. Guerin DJ, Mazeas D, Musale MS, Naguib FNM, Al Safarjalani ON, El Kouni MH, Panzica RP (1999) Uridine phosphorylase inhibitors: chemical modification of benzyloxybenzyl-barbituric acid and its effects on urdpase inhibition. Bioorg Med Chem Lett 9:1477–1480
21. Golovnev NN, Molokeev MS, Vereshchagin SN, Atuchin VV, Sidorenko MY, Dmitrushkov MS (2014) Polyhedron 70:71–76
22. Golovnev NN, Molokeev MS, Vereshchagin SN, Atuchin VV (2013) Calcium and strontium thiobarbiturates with discrete and polymeric structures. J Coord Chem 66:4119–4130
23. Golovnev NN, Molokeev MS, Tarasova LS, Atuchin VV, Vladimirova NI (2014) The 5-(isopropylidene)-2-thiobarbituric acid: Preparation, crystal structure, thermal stability and IR-characterization. J Mol Struct 1068:216–221
24. Golovnev NN, Molokeev MS, Lesnikov MK, Sterkhova IV, Atuchin VV (2017) Thiobarbiturate and barbiturate salts of pefloxacin drug: Growth, structure, thermal stability and IR-spectra. J Mol Struct 1149:367–372
25. Golovnev NN, Molokeev MS, Lesnikov MK, Atuchin VV (2018) Two salts and the salt cocrystal of ciprofloxacin with thiobarbituric and barbituric acids: The structure and properties. J Phys Org Chem 31:e3773
26. Davoll J, Clarke J, Elslager EF (1972) Antimalarial substances. 26. Folate antagonists. 4. Antimalarial and antimetabolite effects of 2, 4-diamino-6-[(benzyl) amino] pyrido [2, 3-d] pyrimidines. J Med Chem 15:837–839
27. Broom AD, Shim JL, Anderson GL (1976) Pyrido [2, 3-d] pyrimidines. IV. Synthetic studies leading to various oxopyrido [2, 3-d] pyrimidines. J Org Chem 41:1095–1099
28. Grivsky EM, Lee S, Sigel CW, Duch DS, Nichol CA (1980) Synthesis and antitumor activity of 2, 4-diamino-6-(2, 5-dimethoxybenzyl)-5-methylpyrido [2, 3-d] pyrimidine. J Med Chem 23:327–329
29. Heber D, Heers C, Ravens U (1993) Positive inotropic activity of 5-amino-6-cyano-1, 3-dimethyl-1, 2, 3, 4-tetrahydropyrido [2, 3-d] pyrim idine-2, 4-dione in cardiac muscle from guinea-pig and man. Part 6: Compounds with positive inotropic activity. Pharmazie 48:537–541
30. Ghorab MM, Hassan AY (1998) Synthesis and antibacterial properties of new dithienyl containing pyran, pyrano [2, 3-b] pyridine, pyrano [2, 3-d] pyrimidine and pyridine derivatives. Phosphorus, Sulfur Relat. Elem. 141:251-261
31. Li JT, Dai HG, Liu D, Li TS (2006) Efficient Method for Synthesis of the Derivatives of 5-Arylidene Barbituric Acid Catalyzed by Aminosulfonic Acid With Grinding. Synth Commun 36:789–794
32. Dewan S, Singh R (2003) One Pot Synthesis of Barbiturates on Reaction of Barbituric Acid with Aldehydes under Microwave Irradiation Using a Variety of Catalysts, Synth. Commun 33:3081–3084
33. Alarreca G, Sanabria R, Miranda R, Arroyo G, Tamariz J, Delgado F (2000) Preparation of Benzylidene Barbituric Acids Promoted by Infrared Irradiation in Absence of Solvent. Synth Commun 30:1295–1301
34. Wang C, Ma J, Zhou X, Zang X, Wang Z, Gao Y, Cui P (2005) 1-n-Butyl-3-Methylimmidazolium Tetrafluoroborate–Promoted Green Synthesis of 5-Arylidene Barbituric Acids and Thiobarbituric Acid Derivatives. Synth Commun 35:2759–2764
35. Vieira AA, Marinho BG, de Souza LG, Fernandes PD, Figueroa-Villar JD (2015) Design, synthesis and in vivo evaluation of sodium 2-benzyl-chloromalonates as new central nervous system depressants. Med Chem Commun 6:1427–1437
36. Figueroa-Villar JD, Vieira AA (2013) "Nuclear magnetic resonance and molecular modeling study of exocyclic carbon–carbon double bond polarization in benzylidene barbiturates". J Mol Struct 1034:310–317
37. Shirini F, Langarudi MSN, Seddighi M, Jolodar OG (2015) Bi-SO_3H functionalized ionic liquid based on DABCO as a mild and efficient catalyst for the synthesis of 1, 8-dioxo-octahydro-xanthene and 5 arylmethylene-pyrimidine-2, 4, 6-trione derivatives. Res Chem Intermed 41:8483–8497
38. Seyyedi N, Shirini F, Langarudi MSN (2016) DABCO-based ionic liquids: green and recyclable catalysts for the synthesis of barbituric and thiobarbituric acid derivatives in aqueous media. RSC Adv 6:44630–44640

39. Mashhadinezhad M, Shirini F, Mamaghani M (2018) Nanoporous Na+-montmorillonite perchloric acid as an efficient heterogeneous catalyst for synthesis of merocyanine dyes based on isoxazolone and barbituric acid. Micropor Mesopor Mat 262:269–282
40. Hosseini H, Sheikhhosseini E, Ghazanfari D (2016) Synthesis of arylidinebarbituric acid derivatives catalyzed by dodecylbenzenesulfonic acid (DBSA) in aqueous media. Iran j catal 6:121–125
41. Kefayati H, Valizadeh M, Islamnezhad A (2014) Green electrosynthesis of pyrano [2, 3-d] pyrimidinones at room temperature. Anal Bioanal Electrochem 6:80–90
42. Hu Y, Chen ZC, Le ZG, Zheng QG (2004) Organic Reactions in Ionic Liquids: Ionic Liquid Promoted Knoevenagel Condensation of Aromatic Aldehydes with (2-Thio) Barbituric Acid. Synth Commun 34:4521–4529
43. Li JT, Sun MX (2009) $SiO_2 \cdot 12WO_3 \cdot 24H_2O$: a highly efficient catalyst for the synthesis of 5-arylidene barbituric acid in the presence of water. Aust J Chem 62:353–355
44. Gadekar LS, Lande MK (2012) Org Chem Ind J 8:386–390
45. Kamble S, Rashinkar G, Kumbhar A, Mote K, Salunkhe R (2010) Green chemistry approach for synthesis of 5-arylidine barbituric acid derivatives by hydrotrope induced Knovenagel condensation in aqueous medium. Arch Appl Sci Res 2:217–222
46. Rajput JK, Kaur G (2013) $CoFe_2O_4$ nanoparticles: An efficient heterogeneous magnetically separable catalyst for “click” synthesis of arylidene barbituric acid derivatives at room temperature. Chin J Catal 34:1697–1704
47. Mirjalili BF, Bamoniri A, Nezamalhosseini SM (2015) BF3/nano-γ-Al_2O_3 Promoted Knoevenagel Condensation at Room Temperature. J Nanostruct 5:3367–3373
48. Abedini M, Shirini F, Omran JMA, Seddighi M, Goli-Jolodar O (2016) Succinimidinium N-sulfonic acid hydrogen sulfate as an efficient ionic liquid catalyst for the synthesis of 5-arylmethylene-pyrimidine-2, 4, 6-trione and pyrano [2, 3-d] pyrimidinone derivatives. Res Chem Intermed 42:4443–4458
49. Khalafinezhad A, Hashemi A (2001) Microwave enhanced Knoevenagel condensation of barbituric acid with aromatic aldehydes on basic alumina. Iran J Chem Chem Eng 20:9–11
50. Safari N, Shirini F, Tajik H (2019) Verjuice as a green and bio-degradable solvent/catalyst for facile and eco-friendly synthesis of 5-arylmethylenepyrimidine-2, 4, 6-trione, pyrano [2, 3-d] pyrimidinone and pyrimido [4, 5-d] pyrimidinone derivatives. J Iran Chem Soc 16:887–897
51. Dighore NR, Anandgaonker PL, Gaikwad ST, Rajbhoj AS (2014) Solvent free green Synthesis of 5-arylidine Barbituric acid Derivatives Catalyzed by Copper oxide Nanoparticles. Res J Chem Sci 4:93–98
52. Thirupathi G, Venkatanarayana M, Dubey PK, Kumari YB (2013) Facile and Green Syntheses of 5-Arylidene-pyrimidine-2, 4, 6-triones and 5-Arylidene-2-thioxo-dihydro-pyrimidine-4, 6-diones Using L-Tyrosine as an Efficient and Eco-Friendly Catalyst in Aqueous Medium. Chem Sci Trans 2:441–446
53. More UB (2016) A Solvent Free Green Protocol for Synthesis of 5-Arylidine Barbituric Acid Derivatives. Org Chem Indian J 12:1–6
54. Khurana JM, Vij K (2010) Nickel nanoparticles catalyzed Knoevenagel condensation of aromatic aldehydes with barbituric acids and 2-thiobarbituric acids. Catal Lett 138:104–110
55. Ren Z, Cao W, Tong W, Jing X (2002) Knoevenagel condensation of aldehydes with cyclic active methylene compounds in water. Synth Commun 32:1947–1952
56. Jin TS, Zhao RQ, Li TS (2007) An Efficient and Convenient Procedure for Preparation of 5-Arylidene Barbituric Acid Catalyzed by ZrO2/SO4-2 Solid Superacid with Grinding. Asian J Chem 19:3815–3820
57. Rathod SB, Gambhire AB, Arbad BR, Lande MK (2010) Synthesis, Characterization and Catalytic Activity of $Ce_1 Mg_x Zr_{1-x} O_2$ (CMZO) Solid Heterogeneous Catalyst for the Synthesis of 5-Arylidine Barbituric acid Derivatives. Bull Korean Chem Soc 31:339–343
58. Daneshvar N, Shirini F, Langarudi MSN, Karimi-Chayjani R (2018) Taurine as a green bio-organic catalyst for the preparation of bio-active barbituric and thiobarbituric acid derivatives in water media. Bioorg Chem 77:68–73
59. Sargazi G, Afzali D, Mostafavi A (2018) A novel synthesis of a new thorium (IV) metal organic framework nanostructure with well controllable procedure through ultrasound assisted reverse micelle method. Ultrason Sonochem 41:234–251
60. Wang H, Wang Q, Teat SJ, Olson DH, Li J (2018) Synthesis, Structure, and Selective Gas Adsorption of a Single-Crystalline Zirconium Based Microporous Metal–Organic Framework. Cryst Growth Des 17:2034–2040
61. Zhang C, Wang QY, Li MD, Zhang GD (2019) Preparation of Submicron Metastable Spherical β-Bi2O3 Particles by Self-Propagating High-Temperature Synthesis Method. J Nanosci Nanotechnol 19:7436–7441
62. Wang X, Feng X, Lu C, Yi G, Jia J, Li H (2018) Mechanical and tribological properties of plasma sprayed NiAl composite coatings with addition of nanostructured TiO_2/Bi_2O_3. Surf Coat Tech 349:157–165
63. Gao X, Shang Y, Liu L, Fu F (2019) Chemisorption-enhanced photocatalytic nitrogen fixation via 2D ultrathin p–n heterojunction AgCl/δ-Bi_2O_3 nanosheets. J Catal 371:71–80
64. Liu S, Wang Y, Ma Z (2018) Bi_2O_3 with Reduced Graphene Oxide Composite as a Supercapacitor Electrode. Int J Electrochem Sci 13:12256–12265
65. Huy BT, Paeng DS, Thao CTB, Phuong NTK, Lee YI (2019) ZnO-Bi_2O_3/graphitic carbon nitride photocatalytic system with H_2O_2-assisted enhanced degradation of Indigo carmine under visible light. Arab J Chem 13:3790–3800
66. Sargazi G, Afzali D, Ebrahimi AK, Badoei-dalfard A, Malekabadi S, Karami Z (2018) Ultrasound assisted reverse micelle efficient synthesis of new Ta-MOF@ Fe_3O_4 core/shell nanostructures as a novel candidate for lipase immobilization. Mater Sci Eng C 93:768–775
67. Daneshvar N, Nasiri M, Shirzad M, Langarudi MSN, Shirini F, Tajik H (2018) The introduction of two new imidazole-based bis-dicationic Bronsted acidic ionic liquids and comparison of their catalytic activity in the synthesis of barbituric acid derivatives. New J Chem 42:9744–9756

68. Darvishzad S, Daneshvar N, Shirini F, Tajik H (2019) Introduction of piperazine-1, 4-diium dihydrogen phosphate as a new and highly efficient dicationic brönsted acidic ionic salt for the synthesis of (thio) barbituric acid derivatives in water. J Mol Struct 1178:420–427
69. Yahyazadehfar M, Sheikhhosseini E, Ahmadi SA, Ghazanfari D (2019) Microwave-associate synthesis of Co_3O_4 nanoparticles as an effcient nanocatalyst for the synthesis of arylidene barbituric and Meldrum's acid derivatives in green media. Appl Organomet Chem 33:e5100
70. Yahyazadehfar M, Ahmadi SA, Sheikhhosseini E, Ghazanfari D (2020) Synthesis of arylidene (thio)barbituric acid derivatives using bentonite as a natural and reusable catalyst in green media. JACR 14:36–34

Figures

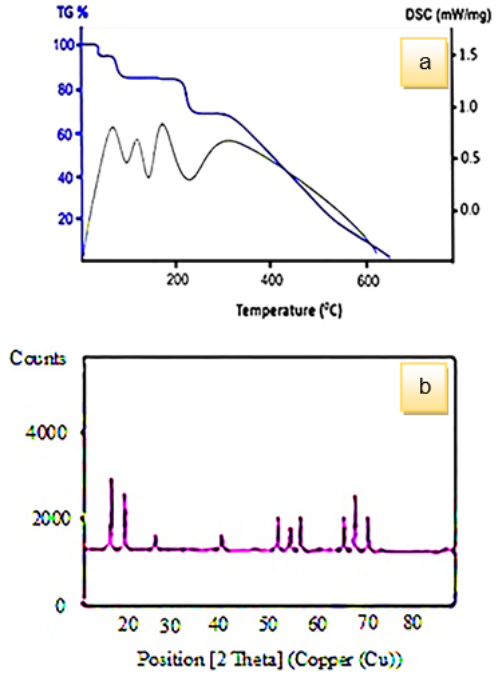

Figure 1

TG and DSC curves (a) and XRD patterns (b) of Bi2O3 nanostructures synthesized under optimal condition of microwave route

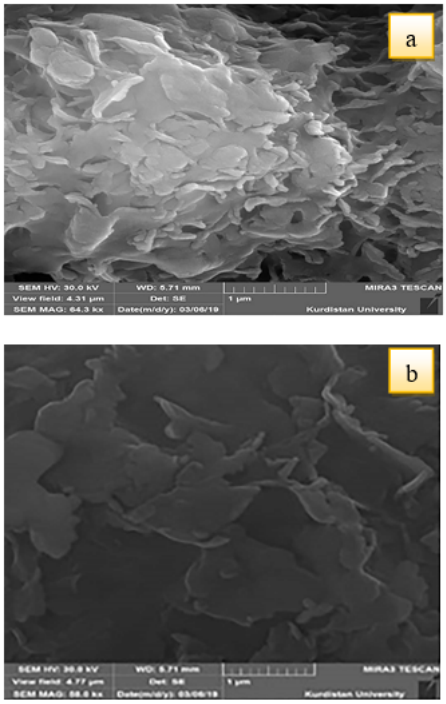

Figure 2

SEM micrograph of the Bi2O3 nanostructure by different magnification (a: 64 kx, and b: 58 kx) synthesized under optimal conditions of the microwave irradiation

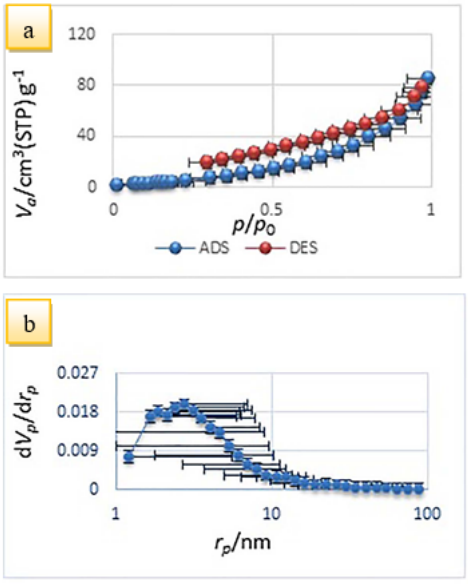

Figure 3

(a) N2 adsorption/desorption isotherm (b) and BJH pore size distribution for Bi2O3 nanostructure

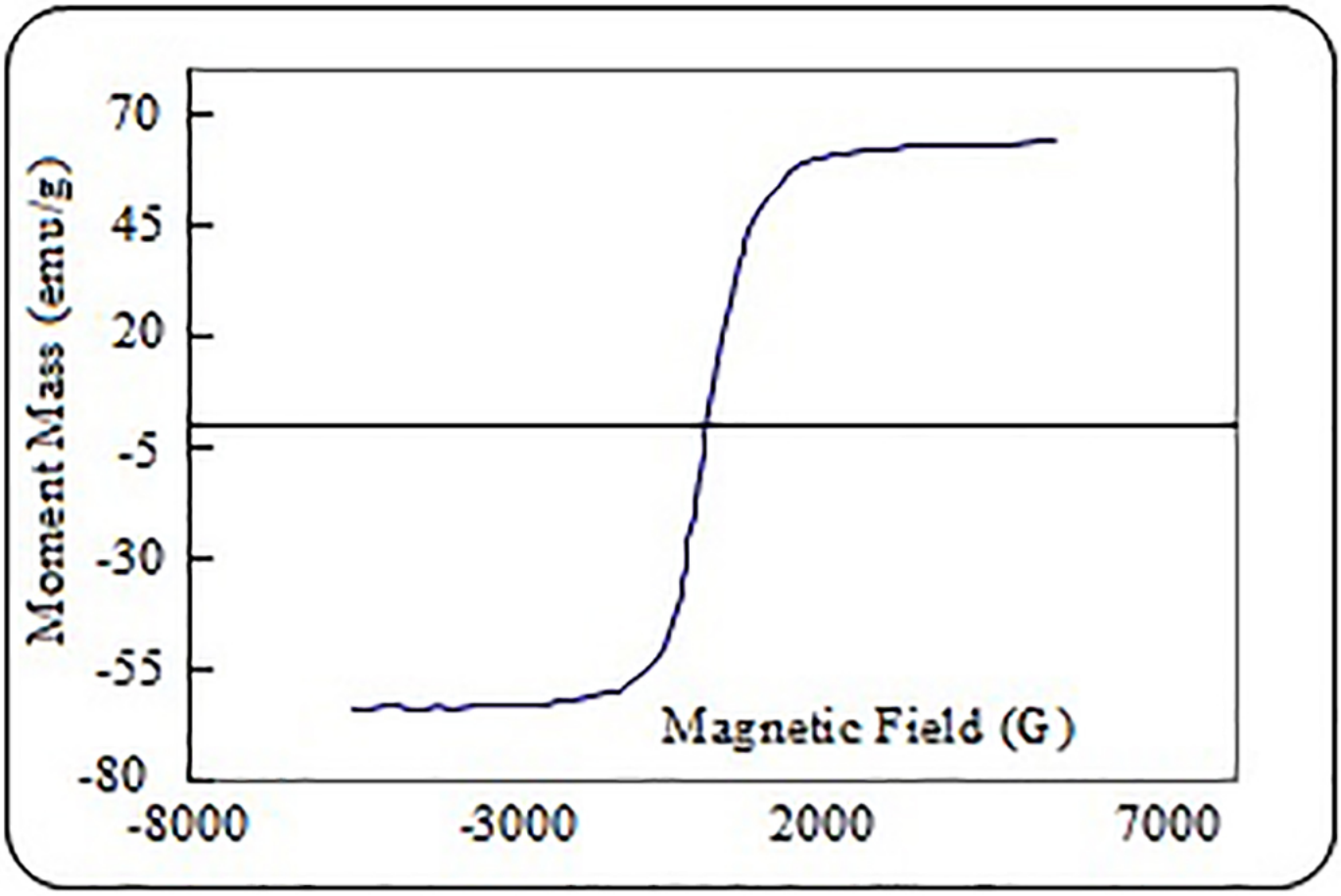

Figure 4

VSM test of Bi2O3 nanostructure synthesized under optimal condition of microwave irradiation

Supplementary Files

This is a list of supplementary files associated with this preprint. Click to download.

- GraphicalAbstract.docx
- Scheme01.png
- Scheme02.png